


Fibroblast cell-based therapy prevents induction of alopecia areata in an experimental model

Cell Transplantation
2018, Vol. 27(6) 994–1004
© The Author(s) 2018
Reprints and permission:
sagepub.com/journalsPermissions.nav
DOI: 10.1177/0963689718773311
journals.sagepub.com/home/ctj


Reza B Jalili¹, Ruhangiz T Kilani¹, Yunyuan Li¹,
Mohsen Khosravi-maharlooie¹, Layla Nabai¹,
Eddy Hsi Chun Wang², Kevin J. McElwee², and Aziz Ghahary¹

Abstract

Alopecia areata (AA) is an autoimmune hair loss disease with infiltration of proinflammatory cells into hair follicles. Current therapeutic regimens are unsatisfactory mainly because of the potential for side effects and/or limited efficacy. Here we report that cultured, transduced fibroblasts, which express the immunomodulatory molecule indoleamine 2,3-dioxygenase (IDO), can be applied to prevent hair loss in an experimental AA model. A single intraperitoneal (IP) injection of IDO-expressing primary dermal fibroblasts was given to C3H/HeJ mice at the time of AA induction. While 60–70% of mice that received either control fibroblasts or vehicle injections developed extensive AA, none of the IDO-expressing fibroblast-treated mice showed new hair loss up to 20 weeks post injection. IDO cell therapy significantly reduced infiltration of CD4⁺ and CD8⁺ T cells into hair follicles and resulted in decreased expression of TNF- α , IFN- γ and IL-17 in the skin. Skin draining lymph nodes of IDO fibroblast-treated mice were significantly smaller, with more CD4⁺ CD25⁺ FoxP3⁺ regulatory T cells and fewer Th17 cells than those of control fibroblast and vehicle-injected mice. These findings indicate that IP injected IDO-expressing dermal fibroblasts can control inflammation and thereby prevent AA hair loss.

Keywords

Alopecia areata, fibroblasts, cell therapy, hair follicles, autoimmunity, immune tolerance, indoleamine 2, 3-dioxygenase

Introduction

Alopecia areata (AA) is a common autoimmune disorder affecting millions of people worldwide. It manifests as a sudden non-scarring loss of hair without visible skin inflammation^{1,2}. Alopecia usually starts abruptly with one or multiple patches of hair loss that usually enlarge in a centrifugal pattern. The entire scalp (alopecia totalis) or body (alopecia universalis) can be affected. Although the exact etiology and pathogenesis of AA are not well understood, loss of immune privilege in hair follicles (HFs) is believed to play a key role in the pathogenesis of AA³. The histopathological finding of peri- and intra-follicular infiltration of CD4⁺ and CD8⁺ lymphocytes, targeting anagen stage HFs, suggests T cell involvement in the pathogenesis of AA. Additionally, the expression of a wide array of proinflammatory cytokines and molecules is associated with collapse of immune privilege in HFs and AA development^{4,5}.

The natural history of AA is unpredictable, which contributes to the devastating nature of the condition and the serious impact it can have on the quality of life of the

patients. No cure currently exists for AA, and available treatments are mainly unsatisfactory either because of lack of efficacy or due to serious side effect potential^{6,7}. Additionally, none of the currently available therapies can prevent future relapse of the disease. Thus, development of an effective, long-lasting treatment is highly desirable for patients suffering from AA.

Our group has recently developed and successfully applied a novel fibroblast cell-based therapy for the treatment of experimental autoimmune type 1 diabetes^{8,9}. We

¹ Department of Surgery, ICORD (international collaboration on regenerative discoveries), University of British Columbia, Canada

² Department of Dermatology and Skin Science, University of British Columbia, Canada

Submitted: July 27, 2017. Revised: March 5, 2018. Accepted: March 9, 2018.

Corresponding Author:

Aziz Ghahary, Burn and Wound Healing Research Lab, 818 W 10th Ave, ICORD, Vancouver, BC V5Z 1M9, Canada.
Email: aghahary@mail.ubc.ca



showed that intraperitoneal (IP) injection of dermal fibroblasts, which expressed the immunomodulatory enzyme indoleamine 2,3-dioxygenase (IDO), to diabetic mice resulted in reinstatement of self-tolerance and subsequent control of autoimmune diabetes. As both type 1 diabetes and AA involve T cell-mediated autoimmunity, here we explored the effect of IDO fibroblast therapy on AA. This was achieved using the C3H/HeJ mouse AA model, which is the most extensively characterized and commonly utilized experimental model for AA^{10–12}. Our results showed that, similarly to type 1 diabetes, IDO fibroblast therapy significantly prevents the development of AA.

Materials and Methods

Experimental mice and IP fibroblast injection

C3H/HeJ mice were obtained from the Jackson Laboratory (Bar Harbor, ME, USA). AA was induced in 8-week-old mice by grafting full-thickness AA-affected C3H/HeJ mouse skin to unaffected mice as described previously¹³. In this model, grafting small pieces of skin from AA-affected to unaffected mice induces onset of AA within 8–10 weeks. It is generally believed that AA-affected mouse skin contains factors capable of inducing AA in immunocompetent hosts by activating host-derived mononuclear cells and triggering an immune response against host HFs. Most likely, activated lymphocytes and/or antigen-presenting cells are transferred with the skin graft and prime naïve host lymphocytes, resulting in induction of AA^{13–15}. To induce AA, in brief, a circular piece of skin about 1.5 cm in diameter was excised from the back of recipient mice and replaced with a full-thickness donor skin graft from mice spontaneously affected with AA. Dermal fibroblasts were explanted from 8–10-week-old C57Bl/6 mouse skin. These fibroblasts (passage 4–5) were then transduced with a lentiviral vector carrying IDO cDNA or a mock vector as described previously¹⁶. IDO-expressing or control fibroblasts (2×10^7 cells/mouse) were injected in a single dose (400 μ l) intraperitoneally (IP) to graft recipient mice on the day of skin grafting.

Histological analyses and immunostainings

Skins of mice were harvested at the endpoint of experiments (20 weeks post-AA induction), kept freshly frozen or fixed in 10% buffered formalin solution, and embedded in paraffin. Tissue sections 5 μ m in thickness were stained with hematoxylin and eosin or rabbit anti-CD3 antibody (1:100 dilution, abcam, Cambridge, MA, USA) then analyzed by light microscopy. Immunofluorescence staining was performed on fresh frozen sections using rat anti-mouse CD4 and CD8 antibodies (1:100 dilution, AbD Serotec, Raleigh, NC, USA). Rhodamine goat anti-rat IgG (Jackson ImmunoResearch, West Grove, PA, USA) was used as the secondary antibody.

Characterization of immune cells

Skin and lymph nodes were harvested at the endpoint of experiments (20 weeks post-AA induction) and single cell suspensions were prepared using collagenase D (Roche Diagnostics, Indianapolis, IN, USA) digestion (1 mg/mL, for 30 min at 37 °C). Cell suspensions were then incubated with fluorescent conjugated antibodies (eBioscience, San Diego, CA, USA) specific for particular lymphocyte markers (i.e. CD4, CD8, CD 25, IL-17, and FoxP3) according to manufacturer's protocol. Fluorescence dot plots were created using the Accuri C6 flow cytometer (BD Biosciences Pharmingen, Mississauga, ON, Canada) and were used to determine the percentage of positive cells labeled with the corresponding antibodies.

Reverse transcriptase polymerase chain reaction (RT-PCR)

Total RNA was isolated from skin tissues using TRIzol (Invitrogen, Carlsbad, CA, USA). The complementary DNA was synthesized by SuperScript II (Invitrogen) using an Oligo (dT) primer (Invitrogen). RT-PCR was performed for 40 cycles at a condition of 95 °C, 30 seconds for denature, 55 °C, 30 seconds for annealing and 68 °C, 40 seconds for replication, using Taq DNA polymerase (New England Biolabs, Whitby, ON, Canada). The following primer sets were used: IL-17 sense (5'-TCCAGAAGGCCCTCAGACTA-3'), IL-17 antisense (5'-AGCATCTTCTCGACCCTGAA-3'), product size: 238 bp; interferon- γ sense (5'-TGCATCTTG GCTTTGCAGCTCTTC-3'), interferon- γ antisense (5'-GGGTTGTTGACCTCAAACCTGGCA3'), product size: 355 bp; TNF- α sense (5'-GAACTGGCAGAAGAGGCACT-3'), TNF- α antisense (5'-AGGGTCTGGGCCATAGAACT-3'), product size: 203 bp; GAPDH sense (5'-GGCATTGCTCT CAATGACAA-3'), GAPDH antisense (5'-TGTGAGGGA GATGCTCAGTG-3'), product size: 200 bp. Amplified PCR products were then separated by 1% agarose gel electrophoresis and visualized with SYBER Safe DNA gel staining (Invitrogen) under UV light.

Cytokine level measurement in skin homogenates using cytometric bead assay

Circular punch samples of skin (6 mm in diameter) were homogenized using a tissue homogenizer in 1 mL of ice-cold cytokine extraction buffer (0.4 M NaCl, 0.05% Tween 20, 0.5% bovine serum albumin, 0.1 mM phenylmethylsulfonyl fluoride, 10 mM EDTA, and 20 Ki of aprotinin). The homogenates were centrifuged at 13,000 \times g for 10 min at 4°C, and supernatants were stored at -80°C before analysis. Interleukin-17A (IL-17), interferon-gamma (IFN- γ), and tumor necrosis factor-alpha (TNF- α) protein levels were quantitatively measured by the BD CBA Mouse Inflammation Kit (BD Bioscience, San Diego, CA, USA). The measurement was performed according to the manufacturer's

instructions. The intensity of the fluorescence signal was acquired on an Accuri C6 flow cytometer and analyzed using FCAP Array Software v3.0 (BD Biosciences).

Tracking intraperitoneal injected fibroblasts

Fibroblasts were labeled using a PKH26 red fluorescent cell membrane labeling kit (Sigma, St. Louis, MO, USA) according to manufacturer's instructions and injected IP into mice. Mice were euthanized at six time points at 7-day intervals (i.e. week 1 to week 6). Cells were retrieved from peritoneal cavity (by lavage), lymph nodes, spleen, lung, and skin. Single cell suspensions from tissues were prepared using collagenase D (Roche Diagnostics) digestion (1 mg/ mL, for 30 min at 37 °C) and examined using flow cytometry. To further characterize the cells that were extracted from lymph nodes, these cells were stained for CD90.2 (eBioscience) and examined using flow cytometry. Presence of migratory fibroblasts in lymph nodes was examined using confocal microscopy. To do so, PKH26-labeled IDO-expressing fibroblasts (2×10^7 cells/mouse) were injected IP into C3 H mice. After 2 weeks, mice were euthanized and mesenteric lymph nodes were harvested, freshly frozen and embedded in Cryomatrix (Thermo Scientific, Kalamazoo, MI, USA). Frozen sections (5 μ m thick) from lymph nodes were permeabilized with 0.1% Triton-X-100 in phosphate buffered saline (PBS), stained with 4',6-diamidino-2-phenylindole (DAPI) and visualized using a confocal fluorescence microscope (Axio Observer Z1 inverted confocal with spinning disk, Carl Zeiss, Jena, Germany). Images were analyzed using Zen software (Carl Zeiss).

Statistical analysis

Data are reported as mean \pm standard deviation of three or more independent sets of experiments. The statistical differences of mean values among treated and control groups were tested with one-way analysis of variance (ANOVA) followed by post hoc comparisons using Bonferroni correction. Kaplan–Meier survival analysis with log-rank (Mantel–Cox) test was done to compare rate of AA incidence among treatment groups. P values less than 0.05 were considered statistically significant.

Results

Alopecia onset was prevented following a single IP injection of IDO-expressing fibroblasts

C3H/HeJ mice (8 weeks old) were induced to develop AA via skin grafting from AA-affected mice as described in the Materials and methods section. On the day of surgery, after the skin grafting procedure, these mice received IP injection of either 2×10^7 IDO-expressing fibroblasts ($n = 15$), control mock vector infected fibroblasts ($n = 10$), or an equivalent volume of cell transfer medium (vehicle, $n = 10$). The

quantity of injected fibroblasts was determined based on the findings of our recent studies showing that 2×10^7 IDO-expressing fibroblasts are sufficient to control autoimmune diabetes^{8–9}. These mice were then monitored weekly for the development of AA. The majority of vehicle and control fibroblast-injected mice started showing AA-like hair loss as early as 8 weeks post-skin grafting. Hair loss typically originated from the ventral side of the body with subsequent extension to the dorsal side in the form of patchy hair loss areas (Figure 1(a) and (b)). In sharp contrast, all IDO fibroblast recipient mice maintained their full pelage coat and none developed AA (Figure 1(c)). Initial skin graft patches on most of the IDO group mice showed hair regrowth, but they remained hairless in a few of the mice. As such, development of AA was defined as the occurrence of hair loss of any size on areas other than the grafted skin site. In total, AA incidence in the vehicle and control fibroblast groups was 70% and 60%, respectively, while no AA case was seen in the IDO fibroblast-treated group in the 20-week follow-up period (Figure 1(d)). Kaplan–Meier plotting with log-rank analysis further confirmed that IDO fibroblast therapy significantly decreased AA incidence ($P < 0.0001$, Figure 1(e)). Overall interpretation of these data indicates that a single IDO fibroblast injection can very effectively prevent AA in C3H/HeJ mice.

IDO fibroblast therapy prevented lymphocyte infiltration and clustering around HFs

At the endpoint of the study, mice were euthanized and their skin was examined using histology and flow cytometry. Hematoxylin and eosin staining revealed typical clustering of mononuclear cells consistent with lymphocyte aggregation around dystrophic HFs in the vehicle and control fibroblast groups, whereas the IDO fibroblast group exhibited healthy HFs with no lymphocyte clustering (Figure 2(a), top row). Further, immunohistological analysis showed CD3⁺ cell accumulation (Figure 2(a), second top row) and the presence of CD4⁺ and CD8⁺ cells (Figure 2(a), two bottom rows) in AA lesions of both vehicle and control fibroblast groups, while no T cells were found around or within HFs of the IDO fibroblast group. To quantify HF infiltrating T cells, skin samples from comparable areas of each group were processed as described in the Materials and methods section, and the resulting cell suspensions were analyzed for CD8 and CD4 T cell markers using flow cytometry (Figure 2(b)). The results, as presented in Figure 2(c), showed that the frequencies of both CD8⁺ and CD4⁺ cells were significantly higher in the skin of vehicle ($13.9\% \pm 1.3\%$ and $8.8\% \pm 1.9\%$, respectively) and control fibroblast groups ($12.8\% \pm 1.8\%$ and $8.4 \pm 1.3\%$, respectively) compared with those of the IDO group ($0.9\% \pm 0.2\%$ and $1.2\% \pm 0.3\%$, respectively, $P < 0.001$, $n = 5$).

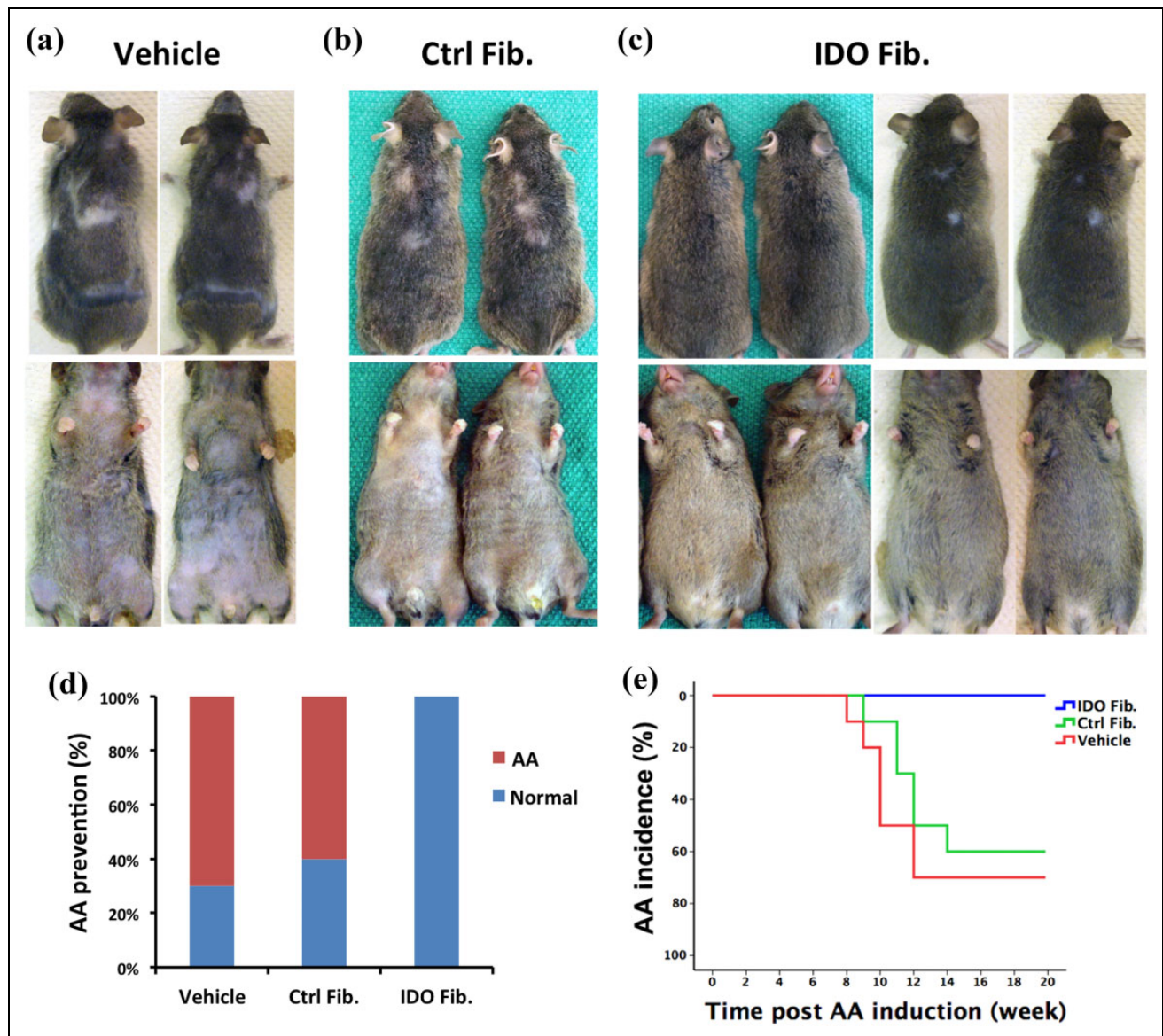


Figure 1. Intra-peritoneal IDO fibroblast injection prevents initiation of AA. IDO-expressing fibroblasts, control fibroblasts, or vehicle solution were injected intra-peritoneally into C3H/HeJ mice at the time of AA induction. Panels (a) to (c) show dorsal and ventral views of representative mice from vehicle, control fibroblast (Ctrl Fib.), and IDO fibroblast (IDO Fib.) injected groups 20 weeks post-AA induction, respectively. Small patches on the back of IDO fib mice are the sites of skin grafting for AA induction. Panel (d): 70% of vehicle and 60% of control fibroblast recipient mice developed extensive AA, while all IDO fibroblast recipient mice remained AA free. Panel (e): Kaplan–Meier survival analysis confirmed significant decrease in AA incidence in the IDO fibroblast-treated group (blue line, $n = 15$) compared with that of vehicle (red line, $n = 10$) and control fibroblast groups (green line, $n = 10$) ($P < 0.0001$).

Skin proinflammatory cytokines expression was prevented by IDO fibroblast therapy

We investigated the inflammatory condition of skin after AA induction in the different treatment groups. To this end, we extracted total RNA from skin and analyzed it using RT-PCR for expression of three major proinflammatory cytokines (TNF- α , IFN- γ , and IL-17). All of the proinflammatory cytokines were highly expressed in both vehicle and control fibroblast groups in an active AA condition, as expected (Figure 3(a)). In contrast, in the IDO fibroblast

group, expression of these cytokines was remarkably reduced. Analysis of RT-PCR results normalized to the glyceraldehyde 3-phosphate dehydrogenase (GAPDH) gene further confirmed the statistically significant lower expression of TNF- α , IL-17, and IFN- γ in the IDO fibroblast group compared with both vehicle and control fibroblast groups (Figure 3(b) to (d)). To further confirm this finding, we measured cytokine levels using the cytokine bead assay as described in the Materials and methods section. The results of the bead assay showed that IFN- γ and IL-17 were undetectable and the TNF- α level was six times lower in skin of

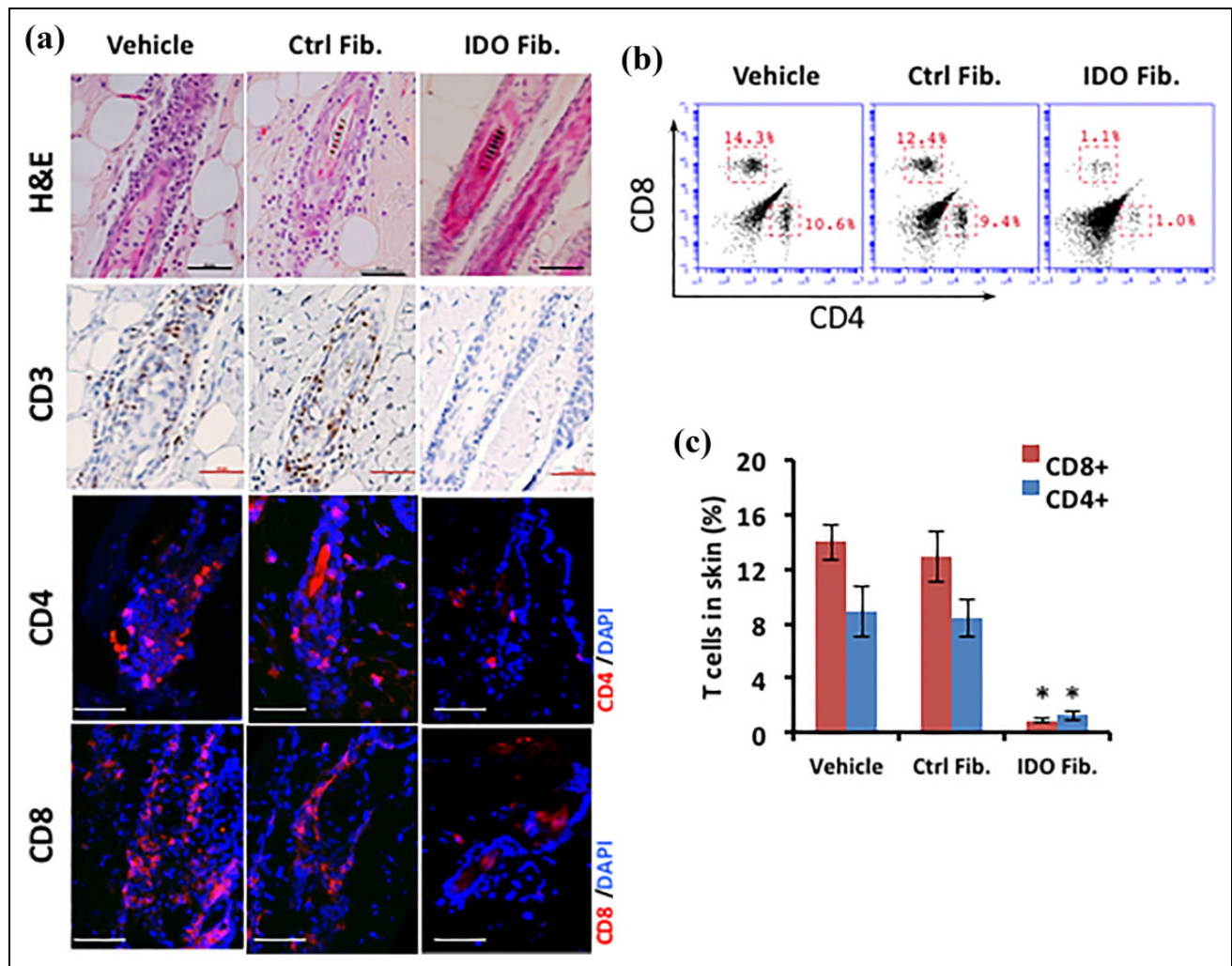


Figure 2. Infiltration of T cells into hair follicles was prevented following IDO fibroblast therapy. IDO-expressing fibroblasts, control fibroblasts, or vehicle solution were injected intraperitoneally into C3H/HeJ mice at the time of AA induction. Panel (a) compares the histology of hair follicles in different treatment groups using hematoxylin and eosin (H&E) staining as well as immune staining for T cell markers including CD3 (brown) CD4 (red), and CD8 (red). Scale bar = 50 μ m. Panel (b) shows representative flow cytometry dot plots for CD4 and CD8 surface markers in skin-derived cells. Panel (c) shows average frequency \pm SD of CD4⁺ and CD8⁺ skin-derived cells in different treatment groups using flow cytometry. *denotes statistically significant difference between IDO and the two other control groups (n = 5, P < 0.001).

the IDO fibroblast-treated group compared with the vehicle and control fibroblast groups (Figure 3 (e) to (g)).

Skin draining lymph nodes exhibited a non-inflammatory state following IDO fibroblast therapy

To gain a perspective on the immune system profile in different treatment groups, we examined axillary and inguinal lymph nodes of mice at the endpoint of the study. The lymph nodes were remarkably larger (Figure 4(a)) and weighed significantly more (Figure 4(b)) in vehicle and control group mice compared with those of the IDO group, suggesting an ongoing active inflammatory condition in the control groups. Further, as shown in Figure 4(c) and (d), flow cytometry analysis of lymphocytes dissociated from lymph nodes

revealed a significantly higher frequency of CD4⁺ CD25⁺ FoxP3⁺ regulatory T cells in the IDO group (10.6% \pm 1.6%) compared with both vehicle (6.3% \pm 1.9%) and control fibroblast groups (6.6% \pm 1.6%, P < 0.01, n = 5). In contrast, the frequency of CD4⁺ IL-17⁺ T cells (compatible with proinflammatory Th17 cells) was significantly lower in the IDO group (3.7% \pm 0.9%) compared with the vehicle (7.4% \pm 2.2%) and control fibroblast groups (7.8% \pm 2.3%, P < 0.05, n = 5) (Figure 4(e) and (f)).

A small population of IP injected fibroblasts migrated to lymph nodes

To investigate the fate of the fibroblasts after IP injection, we labeled IDO-expressing fibroblasts with PKH26 red

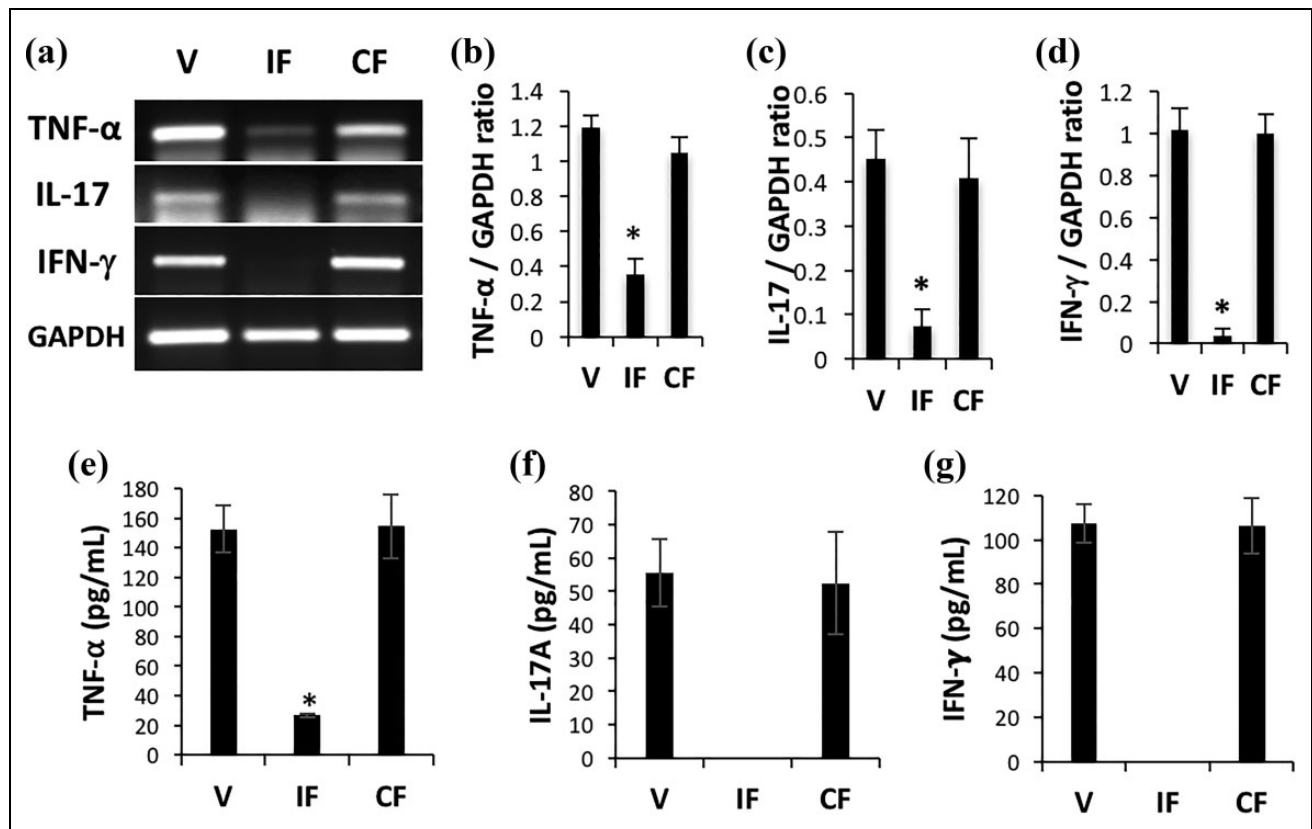


Figure 3. IDO fibroblast therapy resulted in decreased expression of proinflammatory cytokines in skin. IDO-expressing fibroblasts, control fibroblasts, or vehicle solution were injected intraperitoneally into C3H/HeJ mice at the time of AA induction. Total RNA was extracted from skin samples 20 weeks post-AA induction and was analyzed using reverse transcriptase polymerase chain reaction (RT-PCR). Panel (a) shows representative RT-PCR results for TNF- α , IL-17, and IFN- γ in vehicle (V), IDO fibroblast (IF), and control fibroblast (CF) groups. Glyceraldehyde 3-phosphate dehydrogenase (GAPDH) was run as loading control. Panels (b) to (d), respectively, show average relative cytokine mRNA expression \pm SD of TNF- α , IL-17, and IFN- γ in skin of different treatment groups. Panels (e) to (g) show quantitative measurement of these inflammatory cytokines at protein level in skin of different treatment groups using a cytometric bead assay. * denotes statistically significant difference between IDO and the two other control groups ($n = 5$, $P < 0.001$).

fluorescent cell linker. The presence and frequency of IP injected, labeled fibroblasts were then examined in various tissues using flow cytometry 1 week after IP injection. The results showed that IP injected fibroblasts remained primarily in the peritoneal cavity, while a small population migrated to regional draining lymph nodes (Figure 5(a)). No PKH26-labeled cells were found in other tissues, including blood circulation, spleen, lung, or skin. To track fibroblasts homing to lymph nodes, we measured the frequency of PKH26⁺ cells in lymph nodes at different time points after IP injection. We found that PKH26⁺ cells remained in lymph nodes for up to 5 weeks post IP injection, but their frequency decreased over time, and the cells were eventually cleared out after 5 weeks (Figure 5(b)). To visualize the migratory cells within the lymph nodes, frozen sections from C3H mice lymph nodes were examined 2 weeks after IP fibroblast injection using fluorescence confocal microscopy. As shown in Figure 5(c), red PKH26-labeled cells were visible among lymphocytes. To further characterize the phenotype of migratory cells, we co-stained lymph node cells with CD90 as a fibroblast marker. Examining cell surface markers

using flow cytometry at different time points post IP cell injection confirmed that the majority of those PKH26⁺ cells were also CD90 positive (Figure 5(d)). This finding strongly suggests that the PKH26⁺ cells found within lymph nodes are possibly IP injected fibroblasts that migrated to lymph nodes.

Discussion

In this study, we showed that a single IP injection of IDO-expressing fibroblasts very effectively prevented induction of AA in C3H/HeJ mice. AA is one of the most prevalent autoimmune disorders and a major unresolved clinical problem. However, it has not been well studied in comparison to other autoimmune diseases. This gap in information about AA has resulted in a lack of satisfactory and effective treatments. As such, finding novel effective, yet safe, therapeutic methods for AA is greatly needed.

The C3H/HeJ mouse strain is a well-studied experimental model for AA. While only 20% of aged mice develop spontaneous AA^{14,15}, AA can be induced in normal-haired

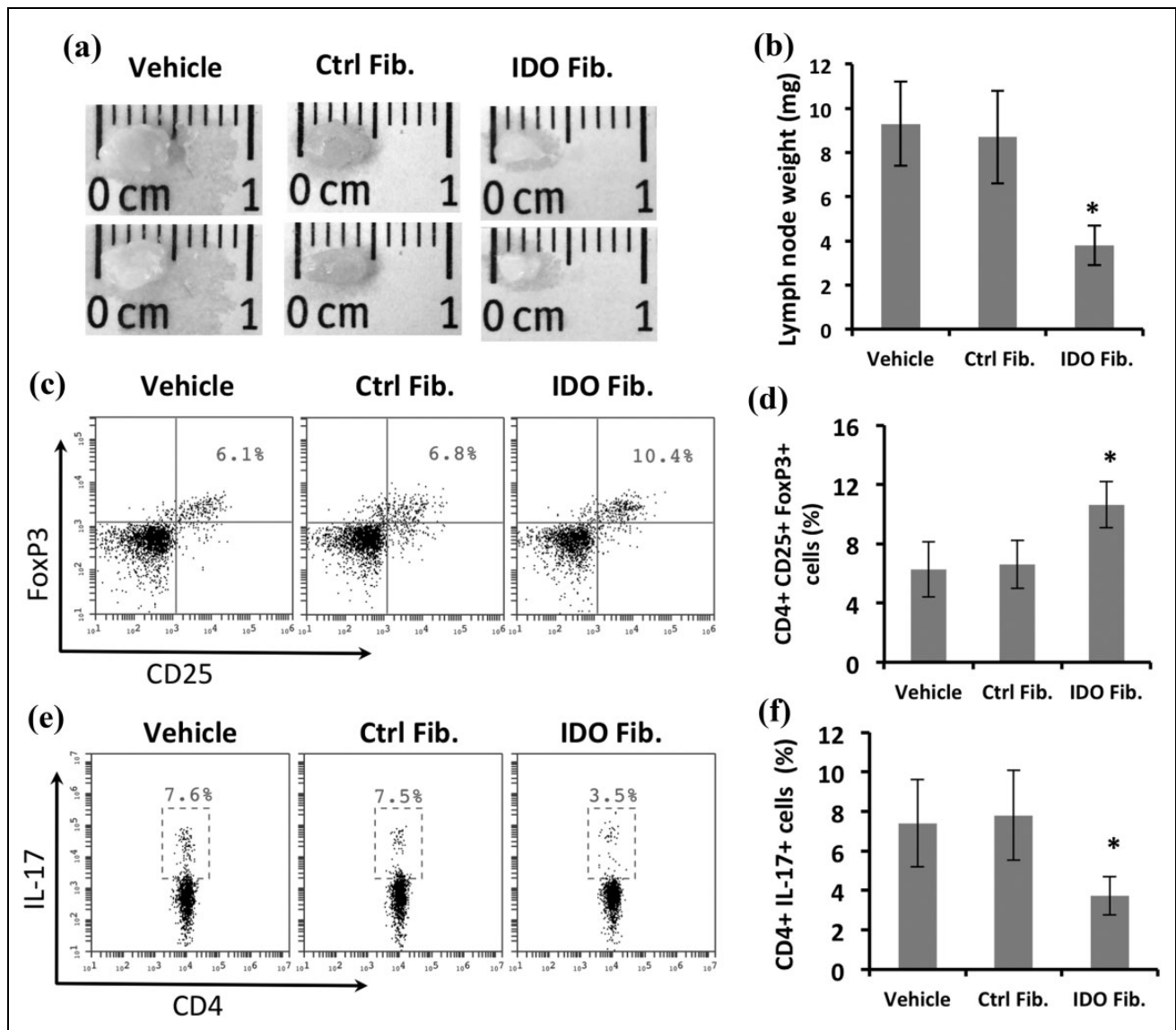


Figure 4. Anti-inflammatory changes in skin draining lymph nodes following IDO fibroblast therapy. IDO-expressing fibroblasts, control fibroblasts, or vehicle solution were injected intraperitoneally into C3H/HeJ mice at the time of AA induction. Panels (a) and (b) show representative axillary and inguinal lymph nodes (LN) size and average weight \pm SD in different treatment groups. Panels (c) and (e), respectively, show representative flow cytometry dot plots for CD25⁺ FoxP3⁺ regulatory T cells, and CD4⁺ IL-17⁺ Th17 cells, both gated on CD4⁺ cells in LN-derived cells. Panels (d) and (f), respectively, show average frequency \pm SD of regulatory T cells and Th17 LN cells in different treatment groups using flow cytometry. *denotes statistically significant difference between IDO and the two other control groups (n = 5, P < 0.01).

C3H/HeJ mice by transplanting a small piece of AA-affected skin¹³ or by intradermal injection of lymph node-derived cells^{17,18}. In this study, we induced AA via grafting full-thickness AA-affected C3H/HeJ mouse skin to unaffected mice. This method usually results in development of AA in 80–100% of mice approximately 8–12 weeks after skin grafting¹³. As shown in Figure 1, while control groups showed a 60–70% rate of extensive AA development, the IDO fibroblast cell-based therapy resulted in a striking prevention of occurrence of new AA lesions in 100% of mice.

Similarly to many other autoimmune diseases, there is a strong body of evidence supporting the role of T cells in the

pathogenesis of AA^{4,19}. Indeed, the most prominent histological characteristic of AA is the perifollicular inflammatory cell infiltration, particularly CD4⁺ and CD8⁺ T cells²⁰. Thus, therapeutic methods that target activated T cells can be considered plausible candidate treatments for AA. The cell-based therapy reported in this study is based on application of dermal fibroblasts that express a potent immunomodulatory enzyme known as IDO. IDO is a rate-limiting enzyme in the tryptophan catabolism pathway, which is a potent regulator of the immune system with a critical function in induction and maintenance of auto- and allo-tolerance^{21,22}.

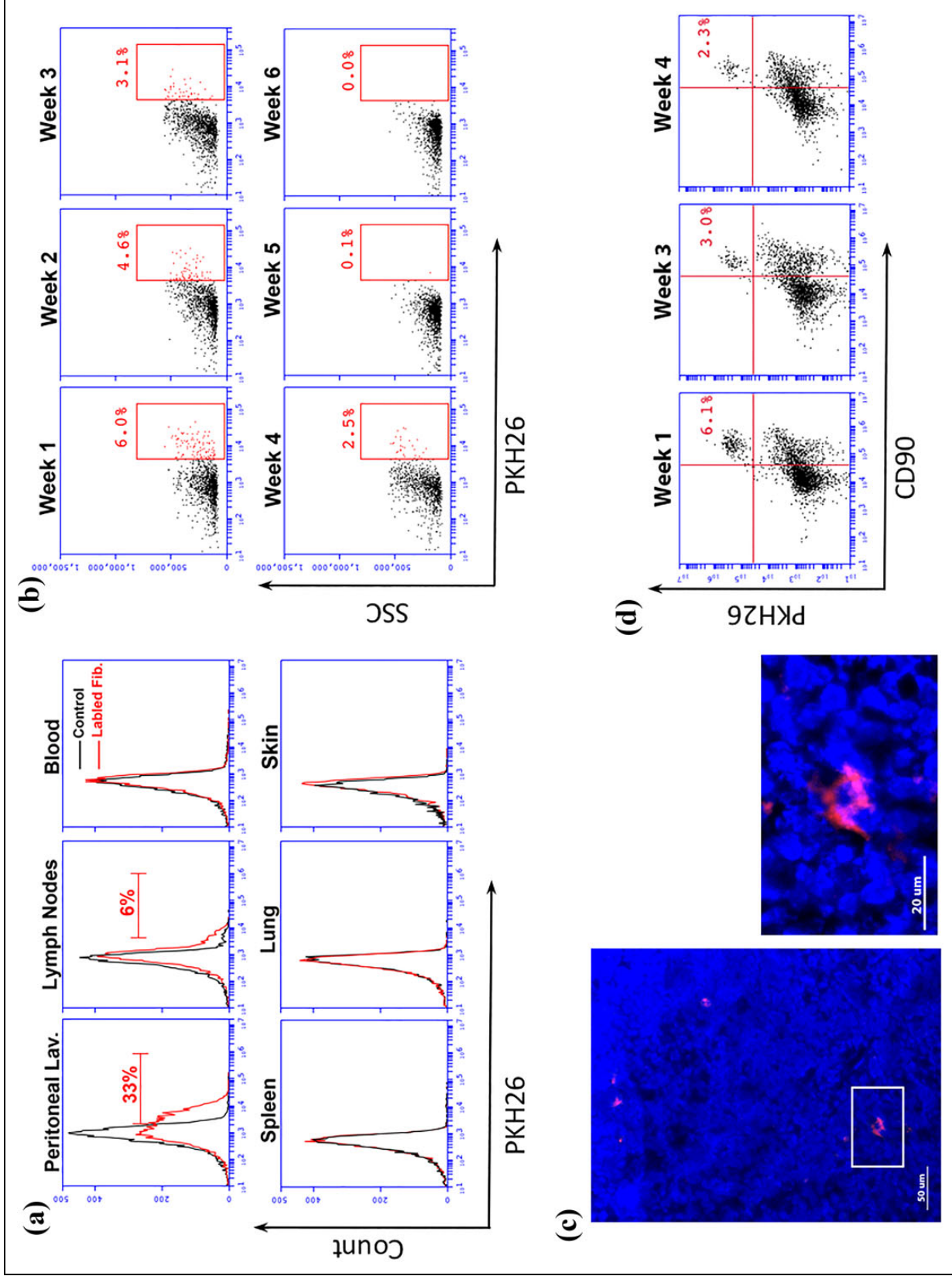


Figure 5. Tracking intraperitoneally (IP) injected fibroblasts. IDO-expressing fibroblasts were labeled with PKH26 red fluorescent cell linker dye and were injected into the peritoneal cavity of C3H/HeJ mice. Migration of these cells to different tissues was then investigated using flow cytometry. Panel (a) shows presence or absence of labeled and control unlabeled fibroblasts 1 week after IP injection in different locations including peritoneal lavage (Lav.), lymph nodes, blood, spleen, lung, and skin. Panel (b) tracks migration and duration of presence of labeled fibroblasts in lymph nodes assessed weekly for a 6-week period. Panel (c) shows a fluorescent micrograph of a sectioned lymph node, 2 weeks following IP injection of labeled IDO fibroblasts. A red fluorescent (PKH26+) cell is shown among lymph node cells with blue colored nuclei (DAPI stained) in low and high magnification. Scale bars in low and high magnification micrographs are 50 and 20 μ m, respectively. Panel (d) shows two-dimensional flow cytometry scatter plots for double positive (PKH26+ and CD90+) cells within lymph nodes at weeks 1, 3, and 4 post IP injection of labeled IDO fibroblasts.

We previously showed that IDO-expressing fibroblasts potentially suppressed activated CD4⁺ and CD8⁺ T cells and significantly increased CD4⁺ CD25⁺ FoxP3⁺ Tregs in different settings^{23–26}. Our findings here (Figure 2) confirm that CD4⁺ and CD8⁺ T cells were significantly prevented from infiltrating into HFs in the IDO group, and therefore hair loss was prevented in these mice. Moreover, we found that prominent proinflammatory cytokines including IFN- γ , TNF- α , and IL-17 were significantly downregulated at both mRNA and protein levels in the IDO fibroblast-treated group. These cytokines are important mediators in AA hair loss induction^{27–32}. Therefore, blocking their production may protect HFs, as we observed in IDO fibroblast-treated mice. Similarly, it has been shown that systemic delivery of other anti-inflammatory treatments such as quercetin by IP injections prevented/reduced the onset of AA, possibly through blocking the expression of proinflammatory cytokines³³.

Another important aspect of IDO's immune regulatory function is its tolerogenic ability. It has been well evidenced that IDO can induce immune tolerance via generating and sustaining the function of regulatory T cells³⁴. In this study, we showed that treatment with IDO fibroblasts resulted in a significant increase in CD4⁺ CD25⁺ FoxP3⁺ Tregs in lymph nodes. These cells are very potent inhibitors of inflammatory and auto-reactive immune cells. In fact, a reduction in the number and function of the Tregs has been reported in AA-affected C3H/HeJ mice³⁵. Accordingly, boosting the quantity and function of Tregs was shown to be beneficial in the treatment of AA³⁶. As such, increased Treg numbers following IDO cell therapy are likely to be a contributing factor in the prevention of AA in this study.

A very important question in this cell therapy model is to elucidate the function and fate of fibroblasts after IP injection. Fibroblasts have long been known as non-professional antigen-presenting cells^{37–40}, and, similarly to mesenchymal stem cells, they can foster an anti-inflammatory condition^{41–43}. Further, we previously showed that IP injected fibroblasts can migrate to lymph nodes and express important co-inhibitory molecules, programmed cell death ligand 1 and 2^{8,44}, which play an important role in suppressing the immune responses in AA⁴⁵ as well as other autoimmune diseases^{46,47}. Therefore, fibroblasts per se can play a role in suppressing destructive immune responses in AA. However, our results in this and previous studies have proven that IDO expression is also required for generating a sufficient tolerance response, as non-IDO-expressing control fibroblasts could not prevent AA.

Regarding the fate of fibroblasts after IP injection, consistently with our previous work^{8,44}, we found that the majority of fibroblasts remain within the peritoneal cavity, with a small fraction migrating to draining lymph nodes. These migratory IDO-expressing fibroblasts homed within lymph nodes for a few weeks and eventually cleared out (Figure 5). The typical 8–12-week delay between the AA trigger event (i.e. skin grafting) and the onset of hair loss suggests that key AA-related immunological events occur before initiation of overt hair loss. It was shown that during

this latent time, proinflammatory events, including lymphocyte priming and proliferation, occur within the lymph nodes prior to significant T cell infiltration into the skin and subsequent hair loss onset^{35,48}. As such, the initial spark for AA onset likely occurs in the draining lymph nodes rather than in the skin. It is possible, therefore, that migratory IDO-expressing fibroblasts interfere with this early proinflammatory process within the lymph nodes and extinguish subsequent propagation of the AA-inducing immune response.

In this study, we did not investigate the effect of IDO cell therapy on treatment of previously established AA lesions. However, as most clinical cases of AA start with the occurrence of a small patch of hair loss^{1,2}, we can speculate that early IDO cell therapy at commencement of the first patch of AA, might be a potentially effective approach for preventing the progression of AA to other regions of the scalp and body. That being said, our group is currently investigating intraleisional injection of IDO-expressing cells for treatment of established AA lesions.

Taken together, the findings of this study show that IDO-expressing fibroblasts can potentially stop autoimmune responses against HFs and very effectively prevent hair loss in an experimental AA model. Although this promising model in its current form may have clear limitations for clinical application, we are optimistic that with further improvements it can open new avenues toward developing an effective AA treatment.

Ethical Approval

University of British Columbia (UBC) Animal Care Committee approved this study (Study ID: A14-0309).

Statement of Human and Animal Rights

University of British Columbia (UBC) Animal Care Committee approved this study (Study ID: A14-0309), and all mice were cared for according to the guidelines of the UBC animal care committee. Mice were kept in standard conditions with all required welfare and full environmental enrichment.

Statement of Informed Consent

Statement of Informed Consent is not applicable for this article.

Declaration of Conflicting Interests

The author(s) declared no potential conflicts of interest with respect to the research, authorship, and/or publication of this article.

Funding

The author(s) disclosed receipt of the following financial support for the research, authorship, and/or publication of this article: This study was supported by the Canadian Institutes of Health Researches (Funding Reference Number: 134214 and 136945).

References

1. Wang E, McElwee KJ. Etiopathogenesis of alopecia areata: why do our patients get it? *Dermatol Ther.* 2011;24(3): 337–347.

2. Hordinsky M, Junqueira AL. Alopecia areata update. *Semin Cutan Med Surg*. 2015;34(2):72–75.
3. Paus R, Bertolini M. The role of hair follicle immune privilege collapse in alopecia areata: status and perspectives. *J Invest Dermatol Symp Proc*. 2013;16(1):S25–S27.
4. McElwee KJ, Gilhar A, Tobin DJ, Ramot Y, Sundberg JP, Nakamura M, Bertolini M, Inui S, Tokura Y, King LE Jr, Duque-Estrad B, Tost A, Keren A, Itami S, Shoenfeld Y, Zlotogorski A, Paus R. What causes alopecia areata? *Exp Dermatol*. 2013;22(9):609–626.
5. Gilhar A, Paus R, Kalish RS. Lymphocytes, neuropeptides, and genes involved in alopecia areata. *J Clin Invest*. 2007;117(8):2019–2027.
6. Iorizzo M, Tosti A. Treatments options for alopecia. *Expert Opin Pharmacother*. 2015;16(15):2343–2354.
7. Santos Z, Avci P, Hamblin MR. Drug discovery for alopecia: gone today, hair tomorrow. *Expert Opin Drug Discov*. 2015;10(3):269–292.
8. Jalili RB, Zhang Y, Hosseini-Tabatabaei A, Kilani RT, Khosravi-Maharlooie M, Li Y, Salimi Elizei S, Warnock GL, Ghahary A. Fibroblast cell-based therapy for experimental autoimmune diabetes. *PLoS One*. 2016;14(11):e0146970.
9. Zhang Y, Jalili RB, Kilani RT, Elizei SS, Farrokhi A, Khosravi-Maharlooie M, Warnock GL, Ao Z, Marzban L, Ghahary A. IDO-expressing fibroblasts protect islet beta cells from immunological attack and reverse hyperglycemia in non-obese diabetic mice. *J Cell Physiol*. 2016; 231(9):1964–1973.
10. Gilhar A, Schrum AG, Etzioni A, Waldmann H, Paus R. Alopecia areata: animal models illuminate autoimmune pathogenesis and novel immunotherapeutic strategies. *Autoimmun Rev*. 2016; 15(7):726–735.
11. McElwee KJ, Freyschmidt-Paul P, Sundberg JP, Hoffmann R. The pathogenesis of alopecia areata in rodent models. *J Invest Dermatol Symp Proc*. 2003;8(1):6–11.
12. McElwee KJ, Hoffmann R. Alopecia areata – animal models. *Clin Exp Dermatol*. 2002;27(5):410–417.
13. McElwee KJ, Boggess D, King LE Jr, Sundberg JP. Experimental induction of alopecia areata-like hair loss in C3H/HeJ mice using full-thickness skin grafts. *J Invest Dermatol*. 1998; 111(5):797–803.
14. Sundberg JP, Cordy WR, King LE Jr. Alopecia areata in aging C3H/HeJ mice. *J Invest Dermatol*. 1994;102(6):847–856.
15. McElwee K, Freyschmidt-Paul P, Ziegler A, Happel R, Hoffmann R. Genetic susceptibility and severity of alopecia areata in human and animal models. *Eur J Dermatol*. 2001;11(1):11–16.
16. Rezakhanlou AM, Habibi D, Lai A, Jalili RB, Ong CJ, Ghahary A. Highly efficient stable expression of indoleamine 2,3 dioxygenase gene in primary fibroblasts. *Biol Proced Online*. 2010; 12(1):9028,010-9028-6.
17. Wang EH, Khosravi-Maharlooie M, Jalili RB, Yu R, Ghahary A, Shapiro J, McElwee KJ. Transfer of alopecia areata to C3H/HeJ mice using cultured lymph node-derived cells. *J Invest Dermatol*. 2015;135(10):2530–2532.
18. Wang EH, McElwee KJ. Induction of alopecia areata in C3H/HeJ mice via cultured cell transfer. *Protoc Exchange*. 2014. doi:10.1038/protex.2014.050.
19. Guo H, Cheng Y, Shapiro J, McElwee K. The role of lymphocytes in the development and treatment of alopecia areata. *Expert Rev Clin Immunol*. 2015;11(12):1335–1351.
20. Islam N, Leung PS, Huntley AC, Gershwin ME. The autoimmune basis of alopecia areata: a comprehensive review. *Autoimmun Rev*. 2015;14(2):81–89.
21. Munn DH, Mellor AL. Indoleamine 2,3 dioxygenase and metabolic control of immune responses. *Trends Immunol* 2013; 34(3):137–143.
22. Mbongue JC, Nicholas DA, Torrez TW, Kim NS, Firek AF, Langridge WH. The role of indoleamine 2, 3-dioxygenase in immune suppression and autoimmunity. *Vaccines (Basel)*. 2015;3(3):703–729.
23. Forouzandeh F, Jalili RB, Germain M, Duronio V, Ghahary A. Differential immunosuppressive effect of indoleamine 2,3-dioxygenase (IDO) on primary human CD4+ and CD8+ T cells. *Mol Cell Biochem*. 2008;309(1–2):1–7.
24. Forouzandeh F, Jalili RB, Hartwell RV, Allan SE, Boyce S, Supp D, Ghahary A. Local expression of indoleamine 2,3-dioxygenase suppresses T-cell-mediated rejection of an engineered bilayer skin substitute. *Wound Repair Regen*. 2010;18(6):614–623.
25. Curran TA, Jalili RB, Farrokhi A, Ghahary A. IDO expressing fibroblasts promote the expansion of antigen specific regulatory T cells. *Immunobiology*. 2014;219(1):17–24.
26. Jalili RB, Forouzandeh F, Rezakhanlou AM, Hartwell R, Medina A, Warnock GL, Larijani B, Ghahary A. Local expression of indoleamine 2,3 dioxygenase in syngeneic fibroblasts significantly prolongs survival of an engineered three-dimensional islet allograft. *Diabetes*. 2010;59(9):2219–2227.
27. Ito T, Tokura Y. The role of cytokines and chemokines in the T-cell-mediated autoimmune process in alopecia areata. *Exp Dermatol*. 2014;23(11):787–791.
28. Atwa MA, Youssef N, Bayoumy NM. T-helper 17 cytokines (interleukins 17, 21, 22, and 6, and tumor necrosis factor-alpha) in patients with alopecia areata: association with clinical type and severity. *Int J Dermatol*. 2016; 55(6):666–672.
29. El-Morsy EH, Eid AA, Ghoneim H, Al-Tameemi KA. Serum level of interleukin-17A in patients with alopecia areata and its relationship to age. *Int J Dermatol*. 2016; 55(8):869–874.
30. Gregoriou S, Papafragkaki D, Kontochristopoulos G, Rallis E, Kalogeromitros D, Rigopoulos D. Cytokines and other mediators in alopecia areata. *Mediators Inflamm*. 2010;2010:928030.
31. Freyschmidt-Paul P, McElwee KJ, Hoffmann R, Sundberg JP, Vitacolonna M, Kissling S, Zoller M. Interferon-gamma-deficient mice are resistant to the development of alopecia areata. *Br J Dermatol*. 2006;155(3):515–521.
32. Ito T, Ito N, Bettermann A, Tokura Y, Takigawa M, Paus R. Collapse and restoration of MHC class-I-dependent immune privilege: exploiting the human hair follicle as a model. *Am J Pathol*. 2004;164(2):623–634.
33. Wikramanayake TC, Villasante AC, Mauro LM, Perez CI, Schachner LA, Jimenez JJ. Prevention and treatment of alopecia areata with quercetin in the C3H/HeJ mouse model. *Cell Stress Chaperones*. 2012;17(2):267–274.

34. Fallarino F, Grohmann U, Puccetti P. Indoleamine 2,3-dioxygenase: from catalyst to signaling function. *Eur J Immunol.* 2012;42(8):1932–1937.
35. Zoller M, McElwee KJ, Engel P, Hoffmann R. Transient CD44 variant isoform expression and reduction in CD4(+)/CD25(+) regulatory T cells in C3H/HeJ mice with alopecia areata. *J Invest Dermatol.* 2002;118(6):983–992.
36. McElwee K, Zoller M, Freyschmidt-Paul P, Hoffmann R. Regulatory T cells in autoimmune diseases and their potential. *J Invest Dermatol Symp Proc.* 2005;10(3):280–281.
37. Kundig TM, Bachmann MF, DiPaolo C, Simard JJ, Battagay M, Lothar H, Gessner A, Kuhlcke K, Ohashi PS, Hengartner H. Fibroblasts as efficient antigen-presenting cells in lymphoid organs. *Science.* 1995;268(5215):1343–1347.
38. Boots AM, Wimmers-Bertens AJ, Rijnders AW. Antigen-presenting capacity of rheumatoid synovial fibroblasts. *Immunology.* 1994;82(2):268–274.
39. Sprent J. Professionals and amateurs. *Curr Biol.* 1995;5(10):1095–1097.
40. Saada JI, Pinchuk IV, Barrera CA, Adegboyega PA, Suarez G, Mifflin RC, Di Mari JF, Reyes VE, Powell DW. Subepithelial myofibroblasts are novel nonprofessional APCs in the human colonic mucosa. *J Immunol.* 2006;177(9):5968–5979.
41. Haniffa MA, Collin MP, Buckley CD, Dazzi F. Mesenchymal stem cells: the fibroblasts' new clothes? *Haematologica.* 2009;94(2):258–263.
42. Jones S, Horwood N, Cope A, Dazzi F. The antiproliferative effect of mesenchymal stem cells is a fundamental property shared by all stromal cells. *J Immunol.* 2007;179(5):2824–2831.
43. Bouffi C, Bony C, Jorgensen C, Noel D. Skin fibroblasts are potent suppressors of inflammation in experimental arthritis. *Ann Rheum Dis.* 2011;70(9):1671–1676.
44. Khosravi-Maharlooei M, Pakyari M, Jalili RB, Salimi-Elizei S, Lai JC, Poormasjedi-Meibod M, Kilani RT, Dutz J, Ghahary A. Tolerogenic effect of mouse fibroblasts on dendritic cells. *Immunology.* 2016;148(1):22–33.
45. Li Y, Yan B, Wang H, Li H, Li Q, Zhao D, Chen Y, Zhang Y, Li W, Zhang J, Wang S, Shen J, Li Y, Guindi E, Zhao Y. Hair regrowth in alopecia areata patients following stem cell educator therapy. *BMC Med.* 2015;13:87.
46. Muenst S, Soysal SD, Tzankov A, Hoeller S. The PD-1/PD-L1 pathway: biological background and clinical relevance of an emerging treatment target in immunotherapy. *Expert Opin Ther Targets.* 2015;19(2):201–211.
47. Fife BT, Pauken KE. The role of the PD-1 pathway in autoimmunity and peripheral tolerance. *Ann N Y Acad Sci.* 2011;1217:45–59.
48. McElwee KJ, Hoffmann R, Freyschmidt-Paul P, Wenzel E, Kissling S, Sundberg JP, Zoller M. Resistance to alopecia areata in C3H/HeJ mice is associated with increased expression of regulatory cytokines and a failure to recruit CD4+ and CD8+ cells. *J Invest Dermatol.* 2002;119(6):1426–1433.